

**Scientific Significance Statement**

We present a unified dataset of co-located benthic littoral nutrient concentrations, sewage indicators, algal and macroinvertebrate community abundance, stable isotopes, and fatty acids from Lake Baikal (Siberia). While researchers have studied Baikal's exceptionally diverse endemic taxa for centuries, this product is the first publicly available dataset of Baikal benthic amphipod species abundance as well as amphipod fatty acid profiles in a machine-readable format with standardized metadata. Furthermore, with over 150 co-located variables, this dataset is the most extensive, publicly available description of Baikal's nearshore benthic communities and food webs. The data are highly structured and incorporate a scripted, sequential workflow, enabling the dataset to either supplement current monitoring efforts or provide data for syntheses across systems.

A unified dataset of co-located sewage pollution, periphyton, and benthic macroinvertebrate community and food web structure from Lake Baikal (Siberia)

Michael F. Meyer<sup>1\*</sup>

Ted Ozersky<sup>2</sup>

Kara H. Woo<sup>3</sup>

Kirill Shchapov<sup>2</sup>

Aaron W. E. Galloway<sup>4</sup>

Julie B. Schram<sup>4</sup>

Daniel D. Snow<sup>5</sup>

Maxim A. Timofeyev<sup>6</sup>

Dmitry Yu. Karnaukhov<sup>6</sup>

Matthew R. Brousil<sup>3</sup>

Stephanie E. Hampton<sup>3</sup>

<sup>1</sup>. School of the Environment, Washington State University, Pullman, WA, USA

<sup>2</sup>. Large Lakes Observatory, University of Minnesota - Duluth, Duluth, MN, USA

<sup>3</sup>. Center for Environmental Research, Education, and Outreach, Washington State University, Pullman, WA, USA

<sup>4</sup>. Oregon Institute of Marine Biology, University of Oregon, Charleston, OR, USA

<sup>5</sup>. School of Natural Resources, University of Nebraska-Lincoln, Lincoln, NE, USA

<sup>6</sup>. Biological Research Institute, Irkutsk State University, Irkutsk, Irkutsk Oblast, Russia

\*corresponding author: michael.f.meyer@wsu.edu

**Author Contribution Statement**

Conceptualized the project: MFM, SEH, TO

Collected samples in the field: MFM, TO, KHW, SEH

Processed samples: MFM, KS, JBS, DDS, TO, AWEG, SEH

Wrote and Reviewed R scripts: MFM, MRB, KHW

Data management: MFM, MRB

Wrote and edited the manuscript: All authors

Approved the final manuscript: All authors

**Grant sponsor information:**

Funding was provided by the National Science Foundation (NSF-DEB-1136637) to S.E.H., a Fulbright Fellowship to M.F.M., a NSF Graduate Research Fellowship to M.F.M. (NSF-DGE-1347973), and the Russian Ministry of Science and Education (N FZZE-2020-0026; N FZZE-2020-0023).

**Key Words:** pharmaceuticals, microplastics, fatty acids, stable isotopes, amphipod, mollusk, diatom, spirogyra

**URL of the Dataset and Metadata with permanent identifier:**

• Environmental Data Initiative:

<https://doi.org/10.6073/pasta/9554b7f19ddd4a614e854f18be978dca>

46 • Open Science Framework: <https://doi.org/10.17605/OSF.IO/9TA8Z>

47  
48 **Code URL with permanent identifier:**

- 49 • Environmental Data Initiative:  
50 <https://doi.org/10.6073/pasta/9554b7f19ddd4a614e854f18be978dca>  
51 • Open Science Framework: <https://doi.org/10.17605/OSF.IO/9TA8Z>

52 **Measurement(s):** Chlorophyll a, Fatty Acids, Pharmaceuticals and Personal Care Products,  
53 Microplastics, Periphyton community abundance, benthic macroinvertebrate abundance, Stable  
54 Isotopes, nitrate, ammonium, total phosphorus  
55 **Technology Type(s):** GC/MS, LC/MS, Spectrophotometry, Fluorometry, Microscopy  
56 **Temporal range:** 19 – 23 August 2015  
57 **Frequency or sampling interval:** single snapshot in time  
58 **Spatial scale:** site-based

59  
60 **Abstract (150 of 150 words)**

61  
62 Sewage released from lakeside development can introduce nutrients and micropollutants that can  
63 restructure aquatic ecosystems. Lake Baikal, the world’s most ancient, biodiverse, and voluminous  
64 freshwater lake, has been experiencing localized sewage pollution from lakeside settlements.  
65 Nearby increasing filamentous algal abundance suggests benthic communities are responding to  
66 localized pollution. We surveyed 40-km of Lake Baikal’s southwestern shoreline 19-23 August  
67 2015 for sewage indicators, including pharmaceuticals, personal care products, and microplastics,  
68 with co-located periphyton, macroinvertebrate, stable isotope, and fatty acid samplings. The data  
69 are structured in a tidy format (a tabular arrangement familiar to limnologists) to encourage reuse.  
70 Unique identifiers corresponding to sampling locations are retained throughout all data files to  
71 facilitate interoperability among the dataset’s 150+ variables. For Lake Baikal studies, these data  
72 can support continued monitoring and research efforts. For global studies of lakes, these data can  
73 help characterize sewage prevalence and ecological consequences of anthropogenic disturbance  
74 across spatial scales.

75  
76 **Background and Motivation**

77  
78 Globally, sewage pollution is a common and often concentrated source of nitrogen and phosphorus  
79 inputs that can reshape aquatic ecosystems. Sewage inputs are often associated with increased  
80 primary production (Edmondson 1970; Moore et al. 2003), which can eventually lead to nuisance  
81 algal blooms (Hall et al. 1999; Lapointe et al. 2015). Even in instances where sewage pollution is  
82 mitigated, restoring systems can be complicated and necessitate system-specific (Jeppesen et al.  
83 2005), long-term mitigation strategies (Hall et al. 1999; Tong et al. 2020). As such, effective  
84 sewage monitoring can require merging a suite of chemical, biological, and ecological data to  
85 synthesize locations and timing of inputs with associated shifts in ecological communities  
86 (Rosenberger et al. 2008; Hampton et al. 2011).

87

Definitively identifying sewage as the source of excess nutrients in a system can be challenging. Nutrients can originate from multiple sources, such as agriculture (Powers et al. 2016) or melting permafrost (Turetsky et al. 2000; Anisimov and Reneva 2006; Moore et al. 2009), which can obfuscate wastewater signals. Unlike nutrients, sewage-specific indicators, such as enhanced  $\delta^{15}\text{N}$  stable isotope signatures (Costanzo et al. 2001; Camilleri and Ozersky 2019), pharmaceuticals and personal care products (PPCPs) (Bendz et al. 2005; Rosi-Marshall and Royer 2012; Meyer et al. 2019) and microplastics (Barnes et al. 2009), can be highly specific to human wastewater. Accordingly, sewage-associated micropollutants have garnered global attention for their usefulness in identifying presence and quantifying magnitude of wastewater inputs. While indicators may accumulate differentially in certain taxa (Gartner et al. 2002; Green 2016; Vendel et al. 2017; Richmond et al. 2018), acutely dangerous concentrations are not common in most aquatic systems (Kolpin et al. 2002; Focazio et al. 2008; Yang et al. 2018). However, chronic exposure to microplastics and PPCPs at even minute concentrations (e.g.,  $\mu\text{g/L}$ ) can still disrupt ecological processes (Richmond et al. 2017). For example, oxazepam can increase feeding rate and decrease sociability of river perch (Brodin et al. 2013), and microplastics can release dissolved organic carbon, thereby altering microbial communities (Romera-Castillo et al. 2018). The pervasiveness and diversity of sewage-associated micropollutants in tandem with their potency as ecologically disrupting compounds necessitates investigation within and across systems, thereby enabling synthesis of how micropollutants alter ecosystems.

When assessing biological responses to increased nutrient loading, littoral benthic algal and macroinvertebrate communities often respond most markedly, as their physical proximity to the shoreline puts them in the path of sewage pollution entering the lake (Rosenberger et al. 2008; Hampton et al. 2011). Filamentous algae, for example, can quickly increase in abundance near sewage sources (Rosenberger et al. 2008; Hampton et al. 2011). As algal communities change, food webs can also restructure. For example, change in algal communities can alter the nutritional value of primary producers or cause changes in the relative abundance of different feeding groups (e.g., increased representation of detritivores). Among the suite of food quality metrics, availability of essential fatty acids (EFAs) offers a nuanced understanding of food quality as primary producers usually maintain consistent EFA signatures (Taipale et al. 2013) and consumers acquire EFAs by grazing (Dalsgaard et al. 2003) or trophic upgrading (Sargent and Falk-Petersen 1988; Dalsgaard et al. 2003).

Together, food web structure, community composition, and sewage indicator data can be powerful tools to assess biological impacts of sewage pollution. Despite their utility, these data are not often available for many limnological systems. PPCPs, for example, have historically been less measured in lake environments (Meyer et al. 2019). In instances where data are available, efficiently merging disparate data into a single, analytically-friendly format can be challenging and sometimes require complex, computationally intensive workflows (Meyer et al. 2020).

To offer a template for harmonizing sewage indicator and biological data, we present a unified data product, which contains disparate data collected from 14 littoral and 3 pelagic sites at Lake Baikal from 19 through 23 August 2015 (Figure 1). Located in Siberia, Lake Baikal is the oldest, most voluminous, and deepest freshwater lake in the world (Hampton et al. 2018). Lake Baikal also has the global distinction of being the most biodiverse lake, with the highest endemism (Moore et al. 2009). The lake is experiencing rapid warming associated with climate change, including decrease

in ice cover duration (Moore et al. 2009), and it exhibits offshore plankton community changes associated with warming (Hampton et al. 2008; Katz et al. 2015; Izmet'seva et al. 2016). Less is known of the change occurring in the nearshore of Lake Baikal, where not only climatic changes (Swann et al. 2020) but also human activity (Timoshkin et al. 2018) may introduce nutrients that alter the environment. Nearshore change is particularly important to understand in Lake Baikal, since the majority of the lake's biodiversity and endemic species occur in the littoral zone (Kozhova and Izmet'seva 1998). While Lake Baikal's pelagic zone is generally ultra-oligotrophic (Yoshida et al. 2003; O'Donnell et al. 2017), littoral areas abutting lakeside settlements have recently shown distinct signs of eutrophication, such as increased filamentous green algae abundance (Timoshkin et al. 2016; Volkova et al. 2018) as well as cyanobacteria (Bondarenko et al. 2021).

As a means of identifying sewage from small, concentrated lakeside towns and the associated ecological responses, we assembled a dataset consisting of over 150 variables collected at 14 littoral and 3 pelagic sampling sites. We structured the dataset in a tidy format, where each row is a sample, each column is a variable, and each CSV file is an observable unit, where more similar variables are contained within an individual file (Wickham 2014). Independent CSV files can be merged using unique locational identifiers as relational keys, enabling future researchers to customize analyses around a particular suite of variables. As a result of the dataset's interoperability, reproducibility, and extensive variable content, it is well poised for future reuse as supporting evidence of sewage pollution in Lake Baikal. Additionally, the data's flexibility and consistent structure enable it to be merged with similar datasets, so as to synthesize biological responses to sewage across systems and scales.

To our knowledge, no raw data on Lake Baikal macroinvertebrates, periphyton, or nearshore water quality are public in a machine-readable format, for any variable (i.e., abundance, fatty acid content, stable isotopes, nutrient and pollutant concentration), and no georeferenced data on pharmaceuticals and personal care products or microplastics appear to be publicly available for any boreal, subarctic, or arctic lakes or rivers in Siberia. Thus, the dataset fills a substantial gap for future studies, providing a window into nearshore biotic assemblages and water quality in a unique, ancient ecosystem that holds 20% of the world's liquid surface water (Moore et al. 2009).

**Data Description**

The final, replicate-level data products are available on the Environmental Data Initiative (EDI), where they can be freely accessed without potential barriers such as paywalls or account registrations (Meyer et al. 2021). The final data are provided as 11 separate CSV files, each structured in a tabular format and containing a "site" column that can be used to merge tables. The repository also contains a compressed folder of R scripts (scripts.tar.gz), which were used in the main analysis of the dataset (Meyer et al., Under Review).

site\_information.csv

This file contains metadata for each of the pelagic and littoral sampling locations. Missing data are assigned as NA.

*year*

180 Year sampling occurred.  
181  
182 *month*  
183 Month sampling occurred.  
184  
185 *day*  
186 Day of month sampling occurred.  
187  
188 *time*  
189 Time sampling occurred as Hours:Minutes.  
190  
191 *site*  
192 Unique alphanumeric identifier for a sampling location.  
193  
194 *lat*  
195 Latitude of sampling location in decimal degrees.  
196  
197 *long*  
198 Longitude of sampling location in decimal degrees.  
199  
200 *site\_description*  
201 Researchers' description of sampling location at the time of sampling.  
202  
203 *distance\_to\_shore\_m*  
204 Distance from *in situ* sampled location to the shoreline in meters.  
205  
206 *depth\_m*  
207 Maximum depth at sampling location in meters.  
208  
209 *air\_temp\_celsius*  
210 Temperature of air at sampling location in Celsius.  
211  
212 *surface\_temp\_celsius*  
213 Temperature of water's surface at sampling location in Celsius.  
214  
215 *mid\_temp\_celsius*  
216 Temperature of water midway (i.e.,  $\text{depth\_m}/2$ ) between surface and bottom at sampling location in  
217 Celsius.  
218  
219 *bottom\_temp\_celsius*  
220 Temperature of water near sediment at sampling location in Celsius.  
221  
222 *comments*  
223 Notes in the field describing sampling conditions.  
224  
225 *shore\_photo*

226 Whether or not photos of the shoreline were taken. Photos are available on the project's Open  
227 Science Framework portal (Meyer et al. 2015).

228  
229 *substrate\_photo*

230 Whether or not photos of the substrate were taken.

231  
232 *sponges*

233 Whether or not sponges were present at a sampling location.

234  
235 *brandtia*

236 Whether or not *Brandtia* spp. (endemic amphipod species) were present at a sampling location.

237  
238 distance\_weighted\_population\_metrics.csv

239  
240 This file contains inverse distance weighted, census-based human population data for each sampled  
241 location. Although the majority of sites do not have adjacent shoreline human developments, we  
242 calculated inverse distance weighted (IDW) population for each sampling location. IDW population  
243 is a generalized representation of the size of and proximity to a sampling location's neighboring  
244 human settlements. As these population estimates are based on census data, they reflect static  
245 populations and do not account for seasonal population deviations from tourism. A full description  
246 of the methods used to calculate IDW population can be found in the companion manuscript Meyer  
247 et al. (Under Review).

248  
249 *site*

250 Unique alphanumeric identifier for a sampling location.

251  
252 *distance\_weighted\_population*

253 Inverse distance weighted population for a given sampling location and estimated as number of  
254 people. Because this interpolation process is a function of the size of and proximity to neighboring  
255 developed sites, values can contain decimal values.

256  
257 nutrients.csv

258  
259 This file contains nutrient concentrations for each of the associated sampling locations. Samples  
260 were collected at a depth of 0.75 m. Nutrient samples were not filtered prior to analysis, meaning  
261 that nitrogen concentrations have the potential to include intracellular nitrogen. Therefore,  
262 nitrogenous species' concentrations may be spurious. Minimal detection limits were estimated as  
263 0.01 mg/L for nitrate, 0.005 mg/L for ammonium, and 0.04 mg/L for phosphorus.

264  
265 *site*

266 Unique alphanumeric identifier for a sampling location.

267  
268 *replicate*

269 Replicate for a given sampling location.

270  
271 *nh4\_mg\_dm3*

272 Ammonium concentration in milligrams of ammonium per cubic decimeter.  
273  
274 *no3\_mg\_dm3*  
275 Nitrate concentration in milligrams of nitrate per cubic decimeter  
276  
277 *tp\_mg\_dm3*  
278 Total phosphorus concentration in milligrams of phosphorus per cubic decimeter.  
279  
280 *tpo43\_mg\_dm3*  
281 Total phosphate concentration as phosphate in milligrams per cubic decimeter.  
282  
283 chlorophylla.csv  
284  
285 This file contains chlorophyll a concentrations in the water column as well as fluorometric  
286 corrections for each littoral and pelagic sampling location. Minimal detection limits were estimated  
287 to be 0.02 mg/L.  
288  
289 *site*  
290 Unique alphanumeric identifier for a sampling location.  
291  
292 *replicate*  
293 Replicate number.  
294  
295 *filtered\_volume\_ml*  
296 Lake water volume filtered in milliliters for a given replicate.  
297  
298 *sample\_volume\_ml*  
299 Sample volume filtered for chlorophyll a extraction.  
300  
301 *raw\_fluo*  
302 Raw, uncorrected fluorometric reading for chlorophyll analysis.  
303  
304 *adjusted\_raw*  
305 Corrected fluorometric reading for chlorophyll analysis.  
306  
307 *chl\_conc*  
308 Chlorophyll a concentration in milligrams per liter.  
309  
310 ppcp.csv  
311  
312 This file contains Pharmaceutical and Personal Care Product (PPCP) concentrations in the water  
313 column at each littoral and pelagic sampling location. Detection limits were estimated to be 0.001  
314 µg/L based on a 500 mL sample volume.  
315  
316 *site*  
317 Unique alphanumeric identifier for a sampling location.



318  
319 *paraxanthine*  
320 Concentration of paraxanthine, also known as 1,7-dimethylxanthine, in micrograms per liter.  
321 Paraxanthine is the main human metabolite of caffeine.  
322  
323 *acetaminophen*  
324 Concentration of acetaminophen, also known as paracetamol, in micrograms per liter.  
325  
326 *amphetamine*  
327 Concentration of amphetamine in micrograms per liter.  
328  
329 *caffeine*  
330 Concentration of caffeine in micrograms per liter.  
331  
332 *carbamazepine*  
333 Concentration of carbamazepine in micrograms per liter.  
334  
335 *cimetidine*  
336 Concentration of cimetidine in micrograms per liter.  
337  
338 *cotinine*  
339 Concentration of cotinine, which is the main human metabolite of nicotine, in micrograms per liter.  
340  
341 *diphenhydramine*  
342 Concentration of diphenhydramine in micrograms per liter.  
343  
344 *mda*  
345 Concentration of methylenedioxyamphetamine in micrograms per liter.  
346  
347 *mdma*  
348 Concentration of methylenedioxymethamphetamine in micrograms per liter.  
349  
350 *methamphetamine*  
351 Concentration of methamphetamine in micrograms per liter.  
352  
353 *morphine*  
354 Concentration of morphine in micrograms per liter.  
355  
356 *phenazone*  
357 Concentration of phenazone in micrograms per liter.  
358  
359 *sulfachloropyridazine*  
360 Concentration of sulfachloropyridazine in micrograms per liter.  
361  
362 *sulfamethazine*  
363 Concentration of *sulfamethazine* in micrograms per liter.

364  
365 *sulfamethoxazole*  
366 Concentration of sulfamethoxazole in micrograms per liter.  
367  
368 *thiabendazole*  
369 Concentration of thiabendazole in micrograms per liter.  
370  
371 *trimethoprim*  
372 Concentration of trimethoprim in micrograms per liter.  
373  
374 *collection\_year*  
375 Year sample was collected in the field.  
376  
377 *collection\_month*  
378 Month sample was collected in the field.  
379  
380 *collection\_day*  
381 Day of month sample was collected in the field.  
382  
383 *analysis\_year*  
384 Year sample was analyzed.  
385  
386 *analysis\_month*  
387 Month sample was analyzed.  
388  
389 *analysis\_day*  
390 Day of month sample was analyzed.  
391  
392 microplastics.csv  
393  
394 This file contains suspended microplastics counts for each of the pelagic and littoral sampling  
395 locations. Although we did not measure microplastic size, our enumeration techniques likely  
396 allowed us to reliably quantify microplastics as small as ~300  $\mu\text{m}$  (Hanvey et al. 2017).  
397  
398 *site*  
399 Unique alphanumeric identifier for a sampling location.  
400  
401 *replicate*  
402 Replicate for a given sampling location. Replicate values of “C” indicate a control.  
403  
404 *fragments*  
405 Number of microplastic fragments observed.  
406  
407 *fibers*  
408 Number of microplastic fibers observed.  
409

410 *beads*  
411 Number of microplastic beads observed.  
412  
413 *comments*  
414 Observer comments while enumerating microplastics.  
415  
416 *volume\_filtered\_ml*  
417 Volume in milliliters for a given replicate filtered.  
418  
419 *periphyton.csv*  
420  
421 This file contains periphyton abundance data, collected from rocks at each of the sampled littoral  
422 locations. For poorly preserved samples, counts are listed as NA for each taxonomic grouping, and  
423 a note in the “comments” column is provided.  
424  
425 *site*  
426 Unique alphanumeric identifier for a sampling location.  
427  
428 *replicate*  
429 Replicate number for a given sampling site.  
430  
431 *subsamples\_counted*  
432 Number of 10 microliter subsamples counted for a given replicate.  
433  
434 *diatom*  
435 Number of diatom cells counted for a given replicate.  
436  
437 *spirogyra*  
438 Number of *Spirogyra* spp. cells counted for a given replicate.  
439  
440 *spirogyra\_filament*  
441 Number of *Spirogyra* spp. filaments counted for a given replicate.  
442  
443 *ulothrix*  
444 Number of *Ulothrix* spp. cells counted for a given replicate.  
445  
446 *ulothrix\_filament*  
447 Number of *Ulothrix* spp. filaments counted for a given replicate.  
448  
449 *tetrasporales*  
450 Number of Tetrasporales cells counted for a given replicate.  
451  
452 *pediastrum*  
453 Number of *Pediastrum* spp. cells counted for a given replicate.  
454  
455 *desmidales*

456 Number of *Desmidales* spp. cells counted for a given replicate.  
457  
458 *comments*  
459 Notes from the observer.  
460  
461 invertebrates.csv  
462  
463 This file contains abundance for benthic macroinvertebrates collected at each of the 14 littoral  
464 sampling locations. Only amphipod taxa were identified to species.  
465  
466 *site*  
467 Unique alphanumeric identifier for a sampling location.  
468  
469 *replicate*  
470 Replicate for sampling location. While three replicates were collected in the field, some samples  
471 were poorly preserved, and invertebrates were not enumerated so as to prevent potential errors.  
472  
473 *Acroloxiidae*  
474 Mollusk family.  
475  
476 *Asellidae*  
477 Isopod family.  
478  
479 *Baicaliidae*  
480 Mollusk family.  
481  
482 *Benedictidae*  
483 Mollusk family.  
484  
485 *Brandtia latissima*  
486 Endemic amphipod species. Three subspecies exist, but samples were not identified to subspecies to  
487 reduce potential errors.  
488  
489 *Brandtia parasitica parasitica*  
490 Endemic amphipod species.  
491  
492 *Caddisflies*  
493 General grouping; specimens were not identified to species.  
494  
495 *Cryptoropus inflatus*  
496 Endemic amphipod species.  
497  
498 *Cryptoropus pachytus*  
499 Endemic amphipod species.  
500  
501 *Cryptoropus rugosus*

- 502 Endemic amphipod species.  
503  
504 *Eulimnogammarus\_capreolus*  
505 Endemic amphipod species.  
506  
507 *Eulimnogammarus\_cruentes*  
508 Endemic amphipod species.  
509  
510 *Eulimnogammarus\_cyaneus*  
511 Endemic amphipod species.  
512  
513 *Eulimnogammarus\_grandimanus*  
514 Endemic amphipod species.  
515  
516 *Eulimnogammarus\_juveniles*  
517 Endemic amphipod genus. Identification kept at genus level so as to prevent misclassification.  
518  
519 *Eulimnogammarus\_maackii*  
520 Endemic amphipod species.  
521  
522 *Eulimnogammarus\_marituji*  
523 Endemic amphipod species.  
524  
525 *Eulimnogammarus\_verucossus*  
526 Endemic amphipod species.  
527  
528 *Eulimnogammarus\_viridis\_viridis*  
529 Endemic amphipod species.  
530  
531 *Eulimnogammarus\_vittatus*  
532 Endemic amphipod species.  
533  
534 *Flatworms*  
535 Not identified beyond phylum.  
536  
537 *Leeches*  
538 Not identified beyond order, although 12 endemic species occur in Lake Baikal.  
539  
540 *Maackia*  
541 Mollusk family.  
542  
543 *Pallasea\_brandtia\_brandtia*  
544 Endemic amphipod species.  
545  
546 *Pallasea\_brandtii\_tenera*  
547 Endemic amphipod species.

548  
549 *Pallasea\_cancelloides*  
550 Endemic amphipod species.  
551  
552 *Pallasea\_cancellus*  
553 Endemic amphipod species.  
554  
555 *Pallasea\_viridis*  
556 Endemic amphipod species.  
557  
558 *Planorbidae*  
559 Mollusk family.  
560  
561 *Poekilogammarus\_crassimus*  
562 Endemic amphipod species.  
563  
564 *Poekilogammarus\_ephippiatus*  
565 Endemic amphipod species.  
566  
567 *Poekilogammarus\_juveniles*  
568 Endemic amphipod genus. Identification kept at genus level so as to prevent misclassification.  
569  
570 *Poekilogammarus\_megonychus\_perpolitus*  
571 Endemic amphipod species.  
572  
573 *Poekilogammarus\_pictus*  
574 Endemic amphipod species.  
575  
576 *Valvatidae*  
577 Mollusk family.  
578  
579 stable\_isotopes.csv  
580  
581 This file contains carbon ( $\delta^{13}\text{C}$ ) and nitrogen ( $\delta^{15}\text{N}$ ) values for various benthic macroinvertebrate  
582 genera and periphyton collected from the 14 littoral sampling locations.  
583  
584 *site*  
585 Unique alphanumeric identifier for a sampling location.  
586  
587 *Genus*  
588 Genus of the analyzed organism.  
589  
590 *Species*  
591 Species of the analyzed organism. When an organism was identified solely to genus, the Species  
592 value is NA.  
593

594 *C13*  
595 Carbon ( $\delta^{13}\text{C}$ ) stable isotope values in parts per thousand.  
596  
597 *N15*  
598 Nitrogen ( $\delta^{15}\text{N}$ ) stable isotope values in parts per thousand.  
599  
600 *comments*  
601 Quality flag column where  $\delta^{13}\text{C}$  samples were outside of the range of standards.  
602  
603 fatty\_acid.csv  
604  
605 This file contains fatty acid concentrations for various benthic macroinvertebrate genera,  
606 periphyton, and endemic *Draparnaldia* spp. benthic algae collected from the 14 littoral sampling  
607 locations.  
608  
609 *site*  
610 Unique alphanumeric identifier for a sampling location.  
611  
612 *Genus*  
613 Genus of the analyzed organism.  
614  
615 *Species*  
616 Species of the analyzed organism. When an organism was identified solely to genus, the Species  
617 value is NA.  
618  
619 *c12\_0*  
620 Concentration of 12:0 fatty acid as micrograms of fatty acid per milligram of tissue.  
621  
622 *i\_14\_0*  
623 Concentration of i-14:0 fatty acid as micrograms of fatty acid per milligram of tissue.  
624  
625 *c14\_0*  
626 Concentration of 14:0 fatty acid as micrograms of fatty acid per milligram of tissue.  
627  
628 *c14\_1w5*  
629 Concentration of 14:1 $\omega$ 5 fatty acid as micrograms of fatty acid per milligram of tissue.  
630  
631 *i\_15\_0*  
632 Concentration of i-15:0 fatty acid as micrograms of fatty acid per milligram of tissue.  
633  
634 *a\_15\_0*  
635 Concentration of a-15:0 fatty acid as micrograms of fatty acid per milligram of tissue.  
636  
637 *c15\_0*  
638 Concentration of 15:0 fatty acid as micrograms of fatty acid per milligram of tissue.  
639

640 *c15\_1w7*  
641 Concentration of 15:1 $\omega$ 7 fatty acid as micrograms of fatty acid per milligram of tissue.  
642  
643 *i\_16\_0*  
644 Concentration of i-16:0 fatty acid as micrograms of fatty acid per milligram of tissue.  
645  
646 *c16\_0*  
647 Concentration of 16:0 fatty acid as micrograms of fatty acid per milligram of tissue.  
648  
649 *c16\_1w9*  
650 Concentration of 16:1 $\omega$ 9 fatty acid as micrograms of fatty acid per milligram of tissue.  
651  
652 *c16\_1w8*  
653 Concentration of 16:1 $\omega$ 8 fatty acid as micrograms of fatty acid per milligram of tissue.  
654  
655 *c16\_1w7*  
656 Concentration of 16:1 $\omega$ 7 fatty acid as micrograms of fatty acid per milligram of tissue.  
657  
658 *c16\_1w6*  
659 Concentration of 16:1 $\omega$ 6 fatty acid as micrograms of fatty acid per milligram of tissue.  
660  
661 *c16\_1w5*  
662 Concentration of 16:1 $\omega$ 5 fatty acid as micrograms of fatty acid per milligram of tissue.  
663  
664 *i\_17\_0*  
665 Concentration of i-17:0 fatty acid as micrograms of fatty acid per milligram of tissue.  
666  
667 *a\_17\_0*  
668 Concentration of a-17:0 fatty acid as micrograms of fatty acid per milligram of tissue.  
669  
670 *c17\_0*  
671 Concentration of 17:0 fatty acid as micrograms of fatty acid per milligram of tissue.  
672  
673 *c17\_1w7*  
674 Concentration of 17:1 $\omega$ 7 fatty acid as micrograms of fatty acid per milligram of tissue.  
675  
676 *c16\_2w7*  
677 Concentration of 16:2 $\omega$ 7 fatty acid as micrograms of fatty acid per milligram of tissue.  
678  
679 *c16\_2w6*  
680 Concentration of 16:2 $\omega$ 6 fatty acid as micrograms of fatty acid per milligram of tissue.  
681  
682 *c16\_2w4*  
683 Concentration of 16:2 $\omega$ 4 fatty acid as micrograms of fatty acid per milligram of tissue.  
684  
685 *c16\_3w6*



686 Concentration of 16:3 $\omega$ 6 fatty acid as micrograms of fatty acid per milligram of tissue.  
687  
688 *c16\_3w4*  
689 Concentration of 16:3 $\omega$ 4 fatty acid as micrograms of fatty acid per milligram of tissue.  
690  
691 *c16\_3w3*  
692 Concentration of 16:3 $\omega$ 3 fatty acid as micrograms of fatty acid per milligram of tissue.  
693  
694 *c16\_4w3*  
695 Concentration of 16:4 $\omega$ 3 fatty acid as micrograms of fatty acid per milligram of tissue.  
696  
697 *c16\_4w1*  
698 Concentration of 16:4 $\omega$ 1 fatty acid as micrograms of fatty acid per milligram of tissue.  
699  
700 *c18\_0*  
701 Concentration of 18:0 fatty acid as micrograms of fatty acid per milligram of tissue.  
702  
703 *c18\_1w9*  
704 Concentration of 18:1 $\omega$ 9 fatty acid as micrograms of fatty acid per milligram of tissue.  
705  
706 *c18\_1w7*  
707 Concentration of 18:1 $\omega$ 7 fatty acid as micrograms of fatty acid per milligram of tissue.  
708  
709 *c18\_2w6t*  
710 Concentration of 18:2 $\omega$ 6t fatty acid as micrograms of fatty acid per milligram of tissue.  
711  
712 *c18\_2w6*  
713 Concentration of 18:2 $\omega$ 6 fatty acid as micrograms of fatty acid per milligram of tissue.  
714  
715 *c18\_3w6*  
716 Concentration of 18:3 $\omega$ 6 fatty acid as micrograms of fatty acid per milligram of tissue.  
717  
718 *c18\_3w3*  
719 Concentration of 18:3 $\omega$ 3 fatty acid as micrograms of fatty acid per milligram of tissue.  
720  
721 *c18\_4w4*  
722 Concentration of 18:4 $\omega$ 4 fatty acid as micrograms of fatty acid per milligram of tissue.  
723  
724 *c18\_4w3*  
725 Concentration of 18:4 $\omega$ 3 fatty acid as micrograms of fatty acid per milligram of tissue.  
726  
727 *c18\_5w3*  
728 Concentration of 18:5 $\omega$ 3 fatty acid as micrograms of fatty acid per milligram of tissue.  
729  
730 *c20\_0*  
731 Concentration of 20:0 fatty acid as micrograms of fatty acid per milligram of tissue.

732  
733 *c20\_1w9*  
734 Concentration of 20:1 $\omega$ 9 fatty acid as micrograms of fatty acid per milligram of tissue.  
735  
736 *c20\_1w7*  
737 Concentration of 20:1 $\omega$ 7 fatty acid as micrograms of fatty acid per milligram of tissue.  
738  
739 *c20\_2w5\_11*  
740 Concentration of 20:2 $\omega$ 5-11 fatty acid as micrograms of fatty acid per milligram of tissue.  
741  
742 *c20\_2w5\_13*  
743 Concentration of 20:2 $\omega$ 5-13 fatty acid as micrograms of fatty acid per milligram of tissue.  
744  
745 *c20\_2w6*  
746 Concentration of 20:2 $\omega$ 6 fatty acid as micrograms of fatty acid per milligram of tissue.  
747  
748 *c20\_3w6*  
749 Concentration of 20:3 $\omega$ 6 fatty acid as micrograms of fatty acid per milligram of tissue.  
750  
751 *c20\_4w6*  
752 Concentration of 20:4 $\omega$ 6 fatty acid as micrograms of fatty acid per milligram of tissue.  
753  
754 *c20\_3w3*  
755 Concentration of 20:3 $\omega$ 3 fatty acid as micrograms of fatty acid per milligram of tissue.  
756  
757 *c20\_4w3*  
758 Concentration of 20:4 $\omega$ 3 fatty acid as micrograms of fatty acid per milligram of tissue.  
759  
760 *c20\_5w3*  
761 Concentration of 20:5 $\omega$ 3 fatty acid as micrograms of fatty acid per milligram of tissue.  
762  
763 *c22\_0*  
764 Concentration of 22:0 fatty acid as micrograms of fatty acid per milligram of tissue.  
765  
766 *c22\_1w9*  
767 Concentration of 22:1 $\omega$ 9 fatty acid as micrograms of fatty acid per milligram of tissue.  
768  
769 *c22\_1w7*  
770 Concentration of 22:1 $\omega$ 7 fatty acid as micrograms of fatty acid per milligram of tissue.  
771  
772 *c22\_2w6*  
773 Concentration of 22:2 $\omega$ 6 fatty acid as micrograms of fatty acid per milligram of tissue.  
774  
775 *c22\_4w6*  
776 Concentration of 22:4 $\omega$ 6 fatty acid as micrograms of fatty acid per milligram of tissue.  
777

778 *c22\_5w6*  
779 Concentration of 22:5 $\omega$ 6 fatty acid as micrograms of fatty acid per milligram of tissue.  
780  
781 *c22\_3w3*  
782 Concentration of 22:3 $\omega$ 3 fatty acid as micrograms of fatty acid per milligram of tissue.  
783  
784 *c22\_4w3*  
785 Concentration of 22:4 $\omega$ 3 fatty acid as micrograms of fatty acid per milligram of tissue.  
786  
787 *c22\_5w3*  
788 Concentration of 22:5 $\omega$ 3 fatty acid as micrograms of fatty acid per milligram of tissue.  
789  
790 *c22\_6w3*  
791 Concentration of 22:6 $\omega$ 3 fatty acid as micrograms of fatty acid per milligram of tissue.  
792  
793 *c24\_0*  
794 Concentration of 24:0 fatty acid as micrograms of fatty acid per milligram of tissue.  
795  
796 *comments*  
797 Quality flag column. Two samples spilled during fatty acid extraction. These samples are flagged as  
798 such. Although concentrations are lower than other samples, proportions between fatty acids are  
799 consistent.  
800  
801 *total\_lipid.csv*  
802  
803 This file contains gravimetry data for each fatty acid sample.  
804  
805 *site*  
806 Unique alphanumeric identifier for a sampling location.  
807  
808 *Genus*  
809 Genus of the analyzed organism.  
810  
811 *Species*  
812 Species of the analyzed organism. When organism was identified solely to genus, the Species value  
813 is NA.  
814  
815 *total\_lipid\_mg\_per\_g*  
816 Total amount of lipids in a sample in milligrams of lipid per gram of tissue.  
817  
818 *deviation*  
819 Samples were weighed three times and standard deviation in measurement was calculated. All  
820 values are reported in milligrams of lipid per gram of tissue.  
821  
822 *comments*

Quality flag column. Two samples spilled during fatty acid extraction. These samples are flagged as such.

## Data Availability

Data are available at the replicate level at the Environmental Data Initiative ([doi.org/10.6073/pasta/9554b7f19ddd4a614e854f18be978dca](https://doi.org/10.6073/pasta/9554b7f19ddd4a614e854f18be978dca)).

## Methods

### *Site Information*

The vast majority of Lake Baikal's 2,100-km shoreline lacks lakeside development (Moore et al. 2009; Timoshkin et al. 2016). Our sample collection focused on a 40-km section of Lake Baikal's southwestern shoreline, which included three settlements of different sizes (Figure 1) during a time of the year when tourism and summertime biological succession were likely at their annual peaks. Littoral locations were chosen to capture a range of sites with varying degrees of adjacent shoreline development – from “developed” (along the waterfront of human settlements) to “undeveloped” (no adjacent human settlements and complete forest cover; Figure 1). The largest, Listvyanka, is primarily a tourist town of approximately 2000 permanent residents, although tourism can contribute significantly to the town's population with approximately 1.2 million annual visitors (Interfax-Tourism 2018). The other two settlements are the villages Bolshie Koty and Bolshoe Goloustnoe, which have approximately 80 and 600 permanent residents, respectively. Bolshie Koty is home to two field research stations and several small tourist accommodations. Bolshoe Goloustnoe has several hotels and tourist camps.

To assess disturbance gradients and ecological responses from littoral-to-pelagic zones and laterally along the shoreline, our transect consisted of 17 sampling sites that were meant to characterize differences along these gradients. Pelagic sites were located 2 to 5 km offshore from each of the developed sites in water depths of 900 to 1300 m (Figure 1; Table 1). All littoral sites were sampled at approximately the same depth (max depth of ~1.25 m) at a distance of 8.90 to 20.75 m from shore (Table 1), which allowed us to collect samples without the need for SCUBA but precluded us from sampling deeper littoral environments. Due to this constraint, only littoral sites contain macroinvertebrate and algal samples. Otherwise, data are available for both littoral and pelagic sites. At each site, air temperature was measured with a mercury thermometer, and photographs were taken of the substrate and the shoreline. Visual inspection of substrate photographs suggested that littoral sites' substrate was consistent among sites and generally was characterized by large, oblate rocks and gravel.

### *Inverse distance weighted (IDW) population calculation for each sampling location*

We recognized that sewage indicator concentrations at each sampling location may be related to a sampling location's spatial position relative to both the size and proximity of neighboring developed sites. Therefore, we created the inverse distance weighted (IDW) population metric to compress, into a single metric, information about human population size, density, and location along the shoreline as well as distance between developed sites and sampling locations.

Our workflow for calculating IDW population required five steps. First, we traced polygons of each lakeside development's perimeter and line geometries of each development's shorelines from satellite imagery for each developed site in Google Earth. Polygons were traced for the entire area of visible development. Similarly, shoreline traces only reflected shoreline length for which there was visible development. Second, polygon and line geometries were downloaded from Google Earth as a .kml file. Third, the .kml file was imported into the R statistical environment (R Core Team 2019), where using the sf package (Pebesma 2018) we calculated shoreline length, polygon area, and centroid location for each developed site. Fourth, we joined point locations of each sampling site with the spatial polygons to calculate the distance from each sampling location to each developed site's centroid. Fifth, we calculated IDW population for each sampling location, using formula (1)

$$(1) I_j = \frac{\frac{P_{LI}}{A_{LI}} * L_{LI}}{D_{j,LI}} + \frac{\frac{P_{BK}}{A_{BK}} * L_{BK}}{D_{j,BK}} + \frac{\frac{P_{BGO}}{A_{BGO}} * L_{BGO}}{D_{j,BGO}}$$

where  $I$  is the IDW population at sampling location  $j$ ,  $P$  is the population at each of the three developed sites Listvyanka (LI), Bolshie Koty (BK), Bolshoe Goloustnoe (BGO),  $A$  is the area of a developed site in  $\text{km}^2$ ,  $L$  is the shoreline length at a developed site in km, and  $D$  is the distance from developed site  $j$  to each developed site's centroid in km. As these population estimates are based on census data, they reflect current, static populations and do not account for seasonal population swings from tourism.

### Nutrients

Water samples for nutrient analyses were collected in 150 mL glass jars that had been washed with phosphate-free soap and rinsed three times with water from the sampling location. Samples were collected at a depth of approximately 0.75 m in duplicates and immediately frozen at  $-20^\circ\text{C}$  until processing at the A. P. Vinogradov Institute of Geochemistry (Siberian Branch of the Russian Academy of Sciences, Irkutsk). Samples were not filtered prior to freezing, meaning that nitrogen and ammonium concentrations may include intracellular nitrogen and overestimate dissolved nitrogenous forms in the water column.

For ammonium (RD:52.24.383-2018 2018) and nitrate (RD:52.24.380-2017 2018) concentrations, samples were analyzed with a spectrophotometer (SF-26). GSO 7258-96 and 7259-96 standards of 1 g/L stock concentration were used to calibrate nitrate and ammonium measurements, respectively. When nitrate and ammonium analyses could be performed within 24 h after thawing, samples were kept at  $2-8^\circ\text{C}$  without addition of preservative agents. When nitrate analyses were performed between 24-48 h after thawing, samples were kept at  $3-5^\circ\text{C}$  and chloroform was added as a preservative at a ratio of 2-4 mL per 1 L of sample volume. When ammonium analyses were performed within 24-96 h after thawing, samples were kept at  $3-5^\circ\text{C}$  and  $\sim 10\%$  sulfuric acid solution was added as a preservative. Phosphorus concentration was measured with a spectrophotometer (SF-46) following the addition of persulfate (GOST:18309-2014 2016). When possible, samples were analyzed within three hours of thawing. When analyses could not be performed within three hours, samples were kept at  $3-5^\circ\text{C}$  and chloroform was added as a preservative at a ratio of 2-4 mL per 1 L of sample volume. Minimal detection limits were estimated as 0.01 mg/L for nitrate, 0.005 mg/L for ammonium, and 0.04 mg/L for phosphorus. Concentrations are reported in mg/L of each analyte.

For comparable methods in English, we recommend data users consult International Standards Organization (ISO) (1984) and ISO (2004) as analogs. Copies of the Russian-language methods are included in the Open Science Framework portal within the directory “Nearshore\_sampling/methods”.

### *Chlorophyll a*

Water samples were collected in 1.5 L plastic bottles from a depth of approximately 0.75 m. Although we did not note the plastic bottles’ materials within the field, all bottles for chlorophyll a measurement were cleaned, beverage bottles and likely made of polyethylene terephthalate. Within 12 h of collection, three subsamples (up to 150 mL each) were filtered through 25-mm diameter, 0.2 µm pore size nitrocellulose filters. Filters were then placed in a 35 mm petri dish, which was wrapped with aluminum foil to prevent light exposure, and frozen in the dark until processing.

Chlorophyll samples were processed in a manner similar to that of Welschmeyer (1994). Nitrocellulose filters were ground in 10 mL of 90% HPLC-grade acetone, in which chlorophyll extraction was allowed to proceed overnight. Chlorophyll extract was then analyzed using a Turner Designs 10-AU fluorometer (Turner Design, Sunnyvale, CA) using an excitation wavelength of 436 nm and emission of 680 nm. 10-AU Secondary Solid Standard (P/N 10-AU-904) was used to calibrate fluorometer prior to samples being processed. Blank samples registered a raw fluorescence of approximately 0.1 FL units. Concentrations were calculated using formula 2 (2)

$$\text{Chlorophyll concentration} = (\text{extract reading} - \text{blank reading}) * \frac{\text{mL of extract}}{\text{mL of filtered sample}}$$

Detection limits are estimated to be approximately 0.02 mg/L. Concentrations are reported as mg/L.

### *Pharmaceuticals and Personal Care Products (PPCPs)*

Water samples for PPCP analysis were collected in 250 mL amber glass bottles that were rinsed with either methanol or acetone and then three times with sample water prior to collections. Following collection, samples were refrigerated and kept in the dark until solid phase extraction (SPE).

Within 12 h of collection, samples were filtered directly from the amber glass bottle using an in-line Teflon filter holder with glass microfiber GMF (1.0 µm pore size, WhatmanGrad 934-AH) in tandem with a solid phase extraction (SPE) cartridge (200 mg HLB, Waters Corporation, Milford, MA) connected to a 1-liter vacuum flask. Lab personnel wore gloves and face masks to minimize contamination. Prior to filtration, SPE cartridges were primed with at least 5 mL of either methanol or acetone and then washed with at least 5 mL of sample water. Rate of extraction was maintained at approximately 1 drop per second. Extraction proceeded until water could no longer pass through the SPE cartridge or until all collected water was filtered. Cartridges were stored in Whirlpacks at -20°C until analysis for 18 PPCP residues using liquid chromatography tandem mass spectrometry (LC-MS-MS) following methods of Lee et al. (2016) and D’Alessio et al (2018) with labeled internal standards (<sup>13</sup>C<sub>3</sub>-caffeine, methamphetamine-d<sub>8</sub>, MDMA-d<sub>8</sub>, morphine-d<sub>3</sub>, and <sup>13</sup>C<sub>6</sub>-sulfamethazine). Detection limits are estimated to be 0.001 µg/L based on a 500 mL sample volume. Concentrations are reported in µg/L.

960 *Microplastics*

961

962 At each location, samples were collected at a depth of approximately 0.75 m in triplicate using 1.5  
963 L clear plastic bottles that were washed thoroughly with sample water before each collection.  
964 Samples were collected by hand for each littoral site and with a metal bucket from aboard the ship  
965 for pelagic sites.

966

967 For processing, each sample was vacuum filtered on to a 47-mm diameter GF/F filter. During  
968 filtration, aluminum foil was used to cover the filtration funnel to prevent contamination from  
969 airborne microplastic particles. After filtration, filters were dried under vacuum pressure and then  
970 stored in 50-mm petri dishes. Following filtration of all three replicates, the filtrate was collected  
971 and then re-filtered through a GF/F filter as a control for contamination from the plastic vacuum  
972 funnel or potentially airborne microplastics.

973

974 Microplastic counting involved visual inspection of the entire GF/F in a similar manner to methods  
975 described in Hanvey et al. (2017). Visual enumeration was conducted under a stereo microscope  
976 with ~100x magnification, and microplastics were classified into one of three categories: fibers,  
977 fragments, or beads. For all categories, plastics were defined as observed objects with apparent  
978 artificial colors, so as to not enumerate plastics potentially contributed from the sampling bottle  
979 itself. Fibers were defined as smooth, long plastics with consistent diameters. Fragments were  
980 defined as plastics with irregularly sharp or jagged edges. Beads were defined as spherical plastics.  
981 Although we did not measure microplastic size, this technique likely allowed us to reliably quantify  
982 microplastics as small as ~300  $\mu\text{m}$  (Hanvey et al. 2017). During enumeration, GF/Fs remained  
983 covered in the petri dish to minimize potential for contamination from the air.

984

985 It is worth noting that since the time of our field sampling, evidence has accumulated that our  
986 methods likely dramatically underestimated microplastic abundance (Wang and Wang 2018;  
987 Brandon et al. 2020). Recent investigations of microplastics in Lake Baikal near Bolshie Koty (BK)  
988 used analogous methods and measured similar microplastic concentrations (Karnaukhov et al.  
989 2020). Future studies aiming to use these data for comparison or supplementing potential data gaps  
990 should consider the minimum microplastic size that could be reliably detected by the method, so as  
991 to ensure data are comparable across methods.

992

993 *Periphyton collection and abundance estimates*

994

995 At each littoral site, we haphazardly selected three rocks representative of local substrate. A plastic  
996 stencil was used to define a surface area of each rock from which we scraped a standardized 14.5  
997  $\text{cm}^2$  patch of periphyton. Samples were preserved with Lugol's solution and stored in plastic  
998 scintillation vials. Additional periphyton was collected in composite from each site for fatty acid  
999 and stable isotope analysis.

1000

1001 Periphyton taxonomic identification and enumeration was performed by subsampling 10  $\mu\text{L}$   
1002 aliquots from each preserved sample, containing approximately 10-15 mL of preserved periphyton.  
1003 For all 10  $\mu\text{L}$  aliquots, cells, filaments, and colonies were counted, for the entire subsample, until at  
1004 least 300 cells were identified for a given sampling replicate. If the first aliquot contained less than  
1005 300 cells, we counted additional subsamples until we reached at least 300 cells in total. In instances

when 300 cells were counted before finishing a subsample, we still counted the entire aliquot. Taxa were classified into broad categories consistent with Baikal algal taxonomy (Izhboldina 2007), using coarse groupings to capture general patterns in relative algal abundance. As a result, algal groups consisted of diatoms, *Ulothrix* spp., *Spirogyra* spp., and the green algal Order Tetrasporales.

Separate periphyton samples for stable isotope and fatty acid analyses were also collected. Instead of preserving samples in Lugol's solution, these samples were immediately frozen at -20°C at the field station. The samples were later transferred to the lab in the U.S. via a Dewar flask with dry ice.

#### *Benthic macroinvertebrate collection and abundance estimates*

Three kick-net samples were collected for assessment of benthic community composition and abundance. Using a D-net, we collected macroinvertebrates by flipping over 1-3 rocks, and then sweeping five times in a left-to-right motion across approximately 1 m. After the series of sweeps, the catch was rinsed into a plastic bucket. For each replicate, bucket contents were concentrated using a 64-µm mesh and placed in glass jars with 40% ethanol (vodka; the only preservative available to us at the time) for preservation and refrigerated at 4°C aboard the research vessel. The 40% ethanol preservative was replaced with ~80% ethanol upon return to the lab within 24 to 48 hours, and samples were stored at ~4°C.

Invertebrate taxonomic identification and enumeration were performed under a stereo microscope. All adult amphipods were identified to species according to Takhteev and Didorenko (2015), whereas juveniles were identified to genus. Mollusks were identified to the family level according to Sitnikova (2012). Leeches were enumerated at the subclass level, but were likely all from the family Glossiphoniidae based on size, depth of sampling locations, and invertebrate communities sampled (Kaygorodova 2012). Like mollusks, caddisflies were also enumerated at the order level, although Baikal does contain over 14 species of caddisfly (Valuyskiy et al. 2020). Flatworms were enumerated at the phylum level. All isopods enumerated were from the family Asellidae. Aside from having limited time available to spend with Baikal taxonomists during our field campaign, our choice of taxonomic resolution ultimately was a result of relative abundance for each taxonomic group, where amphipods were the most abundant taxa and flatworms were among the least abundant taxa across all sites. All samples contained oligochaetes and polychaetes, but due to poor preservation, these taxa were not counted. Six samples of the 42 collected were not well-preserved and were excluded from further analyses, in order to reduce errors in identification. KD-1 and LI-1 were the only sites with 1 sample counted. BK-2 and KD-2 each had two samples counted.

Separate collections were conducted for invertebrate fatty acid and stable isotope analyses. Invertebrates were collected using a D-net and by hand. Organisms collected by hand included amphipod species that were observed from the community composition D-net collections but not readily observed in the stable isotope and fatty acid D-net collections. Collected organisms were live-sorted, identified to species, and then frozen at -20°C at the field station. The samples were later transferred to the lab in the U.S. via a Dewar flask with dry ice.

Due to some samples warming in transit, we only processed samples that were completely frozen upon arrival to the United States. Given the potential for fatty acids to highlight more subtle, multivariate ecological responses along our transect than stable isotopes, we prioritized both



periphyton and macroinvertebrate fatty acid analyses over stable isotope analyses. As such, there is an imbalance across species' abundance, stable isotope, and fatty acid data. Dominant taxa, such as *E. verucosus* and *E. vittatus*, though have paired data throughout the transect, whereas less common taxa, such as *Brandtia* spp., only have abundance estimates. Table 2 summarizes data available for each variable and taxonomic group.

#### *Stable Isotope Analysis*

Following freeze-drying, measurements of periphyton and macroinvertebrate  $\delta^{15}\text{N}$  and  $\delta^{13}\text{C}$  values were performed on an elemental analyzer-isotope ratio mass spectrometer (EA-IRMS; Finnigan DELTAplus XP, Thermo Scientific) at the Large Lakes Observatory, University of Minnesota Duluth. Stable isotope values were calibrated against certified reference materials including L-glutamic acid (NIST SRM 8574), low organic soil and sorghum flour (standards B-2153 and B-2159 from Elemental Micro-analysis Ltd., Okehampton, UK) and in-house standards (acetanilide and caffeine).

#### *Fatty Acid Analysis*

Following freeze-drying, samples were transferred to 10 mL glass centrifuge vials, and 2 mL of 100% chloroform was added to each under nitrogen gas. Samples were allowed to sit in chloroform overnight at  $-80^{\circ}\text{C}$ . Fatty acid extractions generally involved three phases: (1) 100% chloroform extraction, (2) chloroform-methanol extraction, and (3) fatty acid methylation. Fatty acid extraction methods were adapted from Schram et al. (2018).

After overnight chloroform extraction, samples underwent a chloroform-methanol extraction three times. To each sample, we added 1 mL cooled 100% methanol, 1 mL chloroform:methanol solution (2:1), and 0.8 mL 0.9% NaCl solution. Samples were inverted three times and sonicated on ice for 10 minutes. Next, samples were vortexed for 1 minute, and centrifuged for 5 minutes (3,000 rpm) at  $4^{\circ}\text{C}$ . Using a double pipette technique, the lower organic layer was removed and kept under nitrogen. After the third extraction, samples were evaporated under nitrogen flow, and resuspended in 1.5 mL chloroform and stored at  $-20^{\circ}\text{C}$  overnight.

Once resuspended in chloroform, 1 mL of chloroform extract was transferred to a glass centrifuge tube with a glass syringe as well as an internal standard of 4  $\mu\text{L}$  of 19-carbon fatty acid. Samples were then evaporated under nitrogen, and then 1 mL of toluene and 2 mL of 1% sulfuric acid-methanol was added. The vial was closed under nitrogen gas and then incubated in  $50^{\circ}\text{C}$  water bath for 16 hours. After incubation, samples were removed from the bath, allowed to reach room temperature and stored on ice. Next, we performed a potassium carbonate-hexane extraction twice. To each sample, we added 2 mL of 2% potassium bicarbonate and 5 mL of 100% hexane, inverting the capped vial so as to mix the solution. Samples were centrifuged for 3 minutes (1,500 rpm) at  $4^{\circ}\text{C}$ . The upper hexane layer was then removed and placed in a vial to evaporate under nitrogen flow. Once almost evaporated, 1 mL of 100% hexane was added and stored in a glass amber autosampler vial for GC/MS quantification. GC/MS quantification was performed with a Shimadzu QP2020 GC/MS following Schram et al. (2018). As part of our peak quantification protocol, we quantified and identified every lipid compound that showed up in the chromatogram. Each sample contained peaks that were associated with known fatty acids, and among the 59 fatty acids

contained in our dataset, few fatty acids were completely absent from a sample. Consequently, it is difficult for us to definitively ascribe a minimal detection limit to this analysis, but based on standards used, we estimate that this procedure had a minimal detection limit of 1 ng/mL.

Following methylation, remaining extracts were assessed for total lipid masses. Remaining sample extracts (~0.5 mL) were allowed to evaporate to dryness under a fume hood overnight. Dried samples were then left in a weigh room to acclimatize for 30-60 mins and then massed within the scintillation vials. To calculate an average lipid mass, samples were massed three times, so as also to assess deviation in measurements. Lipid gravimetry is reported as the mg of lipids per g of dry-weight tissue.

### Technical Validation

The dataset had three main validation procedures: taxonomic, analytical, and reproducible.

For taxonomic validation, all phylogenetic groupings were based off most recent identification keys. Amphipods were identified according to Takhteev & Didorenko (2015). Mollusks were identified according to Sitnikova (2012). Algal taxa were identified according to Izhboldina (2007). For consistency, all taxa were identified by one person (Michael F. Meyer), who was trained by experts in Baikal algal and macroinvertebrate taxonomy.

For analytical validation, internal standards were used for all mass-spectroscopy analyses. PPCP analyses involved labeled internal standards ( $^{13}\text{C}_3$ -caffeine, methamphetamine-d8, MDMA-d8, morphine-d3, and  $^{13}\text{C}_6$ -sulfamethazine). Stable isotope values were calibrated against certified reference materials including L-glutamic acid (NIST SRM 8574), low organic soil and sorghum flour (standards B-2153 and B-2159 from Elemental Micro-analysis Ltd., Okehampton, UK) and in-house standards (acetanilide and caffeine). Replicate analyses of external standards showed a mean standard deviation of 0.06 ‰ and 0.09 ‰, for  $\delta^{13}\text{C}$  and  $\delta^{15}\text{N}$ , respectively. Finally, fatty acid estimations used an internal 19:0 standard to assess oxidation of fatty acids during extraction, methylation, and quantification.

For data reproducibility, data aggregation and harmonization procedures were conducted in the R statistical environment (R Core Team 2019), using the tidyverse (Wickham et al. 2019) packages. As part of the data aggregation, an initial cleaning script (00\_disaggregated\_data\_cleaning.R) removed incorrect spellings, erroneous data values, and inconsistent column names from raw data. This step created the standardized CSV files detailed above, which are available on the EDI repository (Meyer et al. 2021). Raw data files are available on the project's Open Science Framework portal (Meyer et al. 2015) but are not included in the EDI repository to prevent confusion or incorrect usage. Data hosted on EDI are at the replicate-level but can be aggregated to the sampling-site-level using script "01\_data\_cleaning.R". In addition to aggregation scripts, six R scripts used for analyses in Meyer et al. (*Under Review*) are also available on the EDI repository within the compressed entity "scripts.tar.gz". All R code for data aggregation was written by one person (Michael F. Meyer) and then independently reviewed by two others (Matthew R. Brousil and Kara H. Woo) to confirm that code performed as intended, was well documented, and annotations were complete.

### *A commitment to FAIR and TRUST principles*

Throughout the dataset's development, we strove to incorporate both FAIR (Findable, Accessible, Interoperable, and Reproducible) and TRUST (Transparency, Responsibility, User Focus, Sustainability, and Technology) principles where applicable.

With respect to FAIR principles (Wilkinson et al. 2016), the data are openly accessible in a standardized, replicate-level format on the EDI portal. The 11 CSV files contained within the dataset are entirely interoperable using the "site" column, enabling all variables to efficiently be merged together. Finally, all analytical and some data wrangling scripts are available on the EDI portal in a compressed format, such that future users can reproduce data manipulation and analyses described in Meyer et al. (*Under Review*).

With respect to TRUST principles (Lin et al. 2020), we strove to document additional metadata and data-cleaning practices in a public Open Science Framework (OSF) repository (Meyer et al. 2015). These steps are not necessarily critical to the core EDI dataset, but provide increased transparency for future users wishing recreate the dataset de novo. All "raw" data are provided in the OSF portal, including an initial cleaning script (00\_disaggregated\_data\_cleaning.R) to remove incorrect spellings, erroneous data values, and inconsistent column names. This repository also includes photographs of both field notes as well as photographs of shoreline and substrate from sampling locations. To empower and expedite future reuse, all directories are accompanied with documentation that details directory contents, and all associated scripts are documented and annotated. While many of the files are redundant from the EDI repository, the OSF repository is meant to supplement the EDI repository, so as to enable sustainable, user-focused transparency of how data were collected and cleaned from their raw formats.

### **Data Use and Recommendations for Reuse**

Recognizing the potential for continued low-level, sewage pollution at Lake Baikal (Timoshkin et al. 2016, 2018; Volkova et al. 2018) and lakes worldwide (Yang et al. 2018; Meyer et al. 2019), the final dataset can be applied to a suite of research questions pertaining to ecological responses to human disturbance. We highlight two main areas for immediate application.

First, the final data products can be harmonized with other littoral sampling efforts throughout Lake Baikal, so as to enhance spatial coverage and data diversity. Since 2010, Lake Baikal has experienced increasing filamentous algal abundance, especially near larger lakeside developments (Kravtsova et al. 2014; Timoshkin et al. 2016, 2018; Volkova et al. 2018). Recent benthic algal surveys throughout Lake Baikal's entirety, but especially near our sampling locations, have suggested that cosmopolitan filamentous algae, such as *Spirogyra* spp., tend to be more abundant near larger lakeside developments (Timoshkin et al. 2016; Volkova et al. 2018). For example, Listvyanka is a small town located at the beginning of the Angara River, Lake Baikal's only surface outflow. While Listvyanka's permanent population is approximately 2,000 persons, the town is a growing tourism hub, and hosts over 1.2 million tourists per year (Interfax-Tourism 2018). Surveys conducted near Listvyanka have suggested increased *Spirogyra* spp. abundance is associated with wastewater release (Timoshkin et al. 2016). Although wastewater inputs are likely low and are

1190 diluted to negligible concentrations offshore (Meyer et al., Under Review), combining monitoring  
1191 efforts across spatial and temporal scales are necessary to evaluate the spatial and temporal extent  
1192 of wastewater entering Lake Baikal. As such, our data could complement previous, current, and  
1193 future monitoring efforts, where observations may be missing.  
1194

1195 Second, the final data products are useful to expanding freshwater PPCP, microplastic, and  
1196 associated biological responses across large spatial scales. Recent syntheses of the PPCP literature  
1197 have reported that studies involving lakes are less abundant relative to those focused on lotic  
1198 systems (Meyer et al. 2019). Likewise, microplastic studies have noted that freshwater  
1199 environments are less represented in the literature relative to marine ecosystems (Horton et al.  
1200 2017). For both PPCPs and microplastics, toxic responses to even minute concentrations can be  
1201 uncertain and differ between ecosystem types (e.g., Rosi-Marshall et al. 2013 for lotic and Shaw et  
1202 al. 2015 for lentic). As a result of PPCPs and microplastics garnering increasing attention  
1203 worldwide, sampling of PPCPs and microplastics with co-located biological data across multiple  
1204 spatial and temporal scales would be necessary to synthesize biotic responses to micropollutants  
1205 across systems. Although our data constitute a limited sample number of PPCP and microplastic  
1206 data that exist globally, our final data products are highly structured and flexible for merging with  
1207 similar datasets. Additionally, our dataset's sequential harmonization workflow could be adopted  
1208 by similar monitoring efforts, thereby facilitating data interoperability. Through integration with  
1209 similar monitoring efforts, our dataset can contribute to global synthesis of emerging contaminant  
1210 consequences, especially in a region of the world that is often not easily accessible to many  
1211 researchers.  
1212  
1213

1214 **References**

1215  
1216 Anisimov, O., and S. Reneva. 2006. Permafrost and changing climate: The Russian perspective.  
1217        *Ambio* **35**: 169–175.

1218 Baquero, O. S. 2019. ggsm: North symbols and scale bars for maps created with “ggplot2” or  
1219        “ggmap.”

1220 Barnes, D. K. A., F. Galgani, R. C. Thompson, and M. Barlaz. 2009. Accumulation and  
1221        fragmentation of plastic debris in global environments. *Philos Trans R Soc Lond B Biol Sci*  
1222        **364**: 1985–1998. doi:10.1098/rstb.2008.0205

1223 Bendz, D., N. A. Paxéus, T. R. Ginn, and F. J. Loge. 2005. Occurrence and fate of pharmaceutically  
1224        active compounds in the environment, a case study: Höje River in Sweden. *Journal of*  
1225        *Hazardous Materials* **122**: 195–204. doi:10.1016/j.jhazmat.2005.03.012

1226 Bondarenko, N. A., I. V. Tomberg, A. A. Shirokaya, and others. 2021. *Dolichospermum*  
1227        *lemmermannii* (Nostocales) bloom in world’s deepest Lake Baikal (East Siberia):  
1228        abundance, toxicity and factors influencing growth. *Limnology and Freshwater Biology* **1**:  
1229        1101–1110. doi:10.31951/2658-3518-2021-A-1-1101

1230 Brandon, J. A., A. Freibott, and L. M. Sala. 2020. Patterns of suspended and salp-ingested  
1231        microplastic debris in the North Pacific investigated with epifluorescence microscopy.  
1232        *Limnology and Oceanography Letters* **5**: 46–53. doi:10.1002/lol2.10127

1233 Brodin, T., J. Fick, M. Jonsson, and J. Klaminder. 2013. Dilute concentrations of a psychiatric drug  
1234        alter behavior of fish from natural populations. *Science* **339**: 814–815.  
1235        doi:10.1126/science.1226850

- 1236 Camilleri, A. C., and T. Ozersky. 2019. Large variation in periphyton  $\delta^{13}\text{C}$  and  $\delta^{15}\text{N}$  values in the  
1237 upper Great Lakes: Correlates and implications. *Journal of Great Lakes Research* **45**: 986–  
1238 990. doi:10.1016/j.jglr.2019.06.003
- 1239 Costanzo, S. D., M. J. O'Donohue, W. C. Dennison, N. R. Loneragan, and M. Thomas. 2001. A  
1240 new approach for detecting and mapping sewage impacts. *Marine Pollution Bulletin* **42**:  
1241 149–156. doi:10.1016/S0025-326X(00)00125-9
- 1242 D'Alessio, M., S. Onanong, D. D. Snow, and C. Ray. 2018. Occurrence and removal of  
1243 pharmaceutical compounds and steroids at four wastewater treatment plants in Hawai'i and  
1244 their environmental fate. *Science of The Total Environment* **631–632**: 1360–1370.  
1245 doi:10.1016/j.scitotenv.2018.03.100
- 1246 Dalsgaard, J., M. St. John, G. Kattner, D. Müller-Navarra, and W. Hagen. 2003. Fatty acid trophic  
1247 markers in the pelagic marine environment, p. 225–340. *Advances in Marine Biology*.  
1248 Elsevier.
- 1249 Edmondson, W. T. 1970. Phosphorus, nitrogen, and algae in Lake Washington after diversion of  
1250 sewage. *Science* **169**: 690–691.
- 1251 Fellows, I., and using the Jm. library by J. P. Stotz. 2019. OpenStreetMap: Access to Open Street  
1252 Map Raster Images.
- 1253 Focazio, M. J., D. W. Kolpin, K. K. Barnes, E. T. Furlong, M. T. Meyer, S. D. Zaugg, L. B. Barber,  
1254 and M. E. Thurman. 2008. A national reconnaissance for pharmaceuticals and other organic  
1255 wastewater contaminants in the United States - II) Untreated drinking water sources.  
1256 *Science of the Total Environment* **402**: 201–216. doi:10.1016/j.scitotenv.2008.02.021

- 1257 Gartner, A., P. Lavery, and A. J. Smit. 2002. Use of  $\delta\text{N-15}$  signatures of different functional forms  
1258 of macroalgae and filter-feeders to reveal temporal and spatial patterns in sewage dispersal.  
1259 Mar. Ecol.-Prog. Ser. **235**: 63–73. doi:10.3354/meps235063
- 1260 GOST:18309-2014. 2016. Methods for determination of phosphorus-containing matters (with  
1261 corrections) (Методы определения фосфорсодержащих веществ).
- 1262 Green, D. S. 2016. Effects of microplastics on European flat oysters, *Ostrea edulis* and their  
1263 associated benthic communities. Environmental Pollution **216**: 95–103.  
1264 doi:10.1016/j.envpol.2016.05.043
- 1265 Hall, R. I., P. R. Leavitt, R. Quinlan, A. S. Dixit, and J. P. Smol. 1999. Effects of agriculture,  
1266 urbanization, and climate on water quality in the northern Great Plains. Limnology and  
1267 Oceanography **44**: 739–756. doi:10.4319/lo.1999.44.3\_part\_2.0739
- 1268 Hampton, S. E., S. C. Fradkin, P. R. Leavitt, and E. E. Rosenberger. 2011. Disproportionate  
1269 importance of nearshore habitat for the food web of a deep oligotrophic lake. Marine and  
1270 Freshwater Research **62**: 350. doi:10.1071/MF10229
- 1271 Hampton, S. E., L. R. Izmet'Eva, M. V. Moore, S. L. Katz, B. Dennis, and E. A. Silow. 2008.  
1272 Sixty years of environmental change in the world's largest freshwater lake - Lake Baikal,  
1273 Siberia. Global Change Biology **14**: 1947–1958. doi:10.1111/j.1365-2486.2008.01616.x
- 1274 Hampton, S. E., S. McGowan, T. Ozersky, and others. 2018. Recent ecological change in ancient  
1275 lakes. Limnology and Oceanography **63**: 2277–2304. doi:10.1002/lno.10938
- 1276 Hanvey, J. S., P. J. Lewis, J. L. Lavers, N. D. Crosbie, K. Pozo, and B. O. Clarke. 2017. A review  
1277 of analytical techniques for quantifying microplastics in sediments. Anal. Methods **9**: 1369–  
1278 1383. doi:10.1039/C6AY02707E

- 1279 Horton, A. A., A. Walton, D. J. Spurgeon, E. Lahive, and C. Svendsen. 2017. Microplastics in  
1280 freshwater and terrestrial environments: Evaluating the current understanding to identify the  
1281 knowledge gaps and future research priorities. *Science of The Total Environment* **586**: 127–  
1282 141. doi:10.1016/j.scitotenv.2017.01.190
- 1283 Interfax-Tourism. 2018. Байкал с января по август 2018 года посетили 1,2 миллиона туристов  
1284 (1.2 million tourists vistied Baikal from January through August 2018). Interfax-Tourism,  
1285 October 25
- 1286 International Standards Organization (ISO). 1984. ISO 6777:1984(en) Water quality —  
1287 Determination of nitrite — Molecular absorption spectrometric method. ISO 6777. ISO  
1288 6777 ISO.
- 1289 International Standards Organization (ISO). 2004. ISO 6878:2004(en) Water quality —  
1290 Determination of phosphorus — Ammonium molybdate spectrometric method. ISO 6878.  
1291 ISO 6878 ISO.
- 1292 Izhboldina, L. A. 2007. Guide and Key to Benthic and Periphyton Algae of Lake Baikal (meio- and  
1293 macrophytes) with Brief Notes on Their Ecology, Nauka-Centre.
- 1294 Izmet'seva, L. R., M. V. Moore, S. E. Hampton, and others. 2016. Lake-wide physical and  
1295 biological trends associated with warming in Lake Baikal. *Journal of Great Lakes Research*  
1296 **42**: 6–17. doi:10.1016/j.jglr.2015.11.006
- 1297 Jeppesen, E., M. Søndergaard, J. P. Jensen, and others. 2005. Lake responses to reduced nutrient  
1298 loading – an analysis of contemporary long-term data from 35 case studies. *Freshwater*  
1299 *Biology* **50**: 1747–1771. doi:10.1111/j.1365-2427.2005.01415.x



- 1300 Karnaukhov, D., S. Biritskaya, E. Dolinskaya, M. Teplykh, N. Silenko, Y. Ermolaeva, and E.  
1301 Silow. 2020. Pollution by macro- and microplastic of large lacustrine ecosystems in Eastern  
1302 Asia. *Pollution Research* **2**: 353–355.
- 1303 Kassambara, A. 2019. ggpubr: “ggplot2” Based Publication Ready Plots.
- 1304 Katz, S. L., L. R. Izmet’s’eva, S. E. Hampton, T. Ozersky, K. Shchapov, M. V. Moore, S. V.  
1305 Shimaraeva, and E. A. Silow. 2015. The “Melosira years” of Lake Baikal: Winter  
1306 environmental conditions at ice onset predict under-ice algal blooms in spring. *Limnology*  
1307 *and Oceanography* **60**: 1950–1964. doi:10.1002/lno.10143
- 1308 Kolpin, D. W., E. T. Furlong, M. T. Meyer, E. M. Thurman, S. D. Zaugg, L. B. Barber, and H. T.  
1309 Buxton. 2002. Pharmaceuticals, hormones, and other organic wastewater contaminants in  
1310 U.S. Streams, 1999–2000: A national reconnaissance. *Environmental Science &*  
1311 *Technology* **36**: 1202–1211. doi:10.1021/es011055j
- 1312 Kozhova, O. M., and L. R. Izmet’s’eva. 1998. *Lake Baikal: Evolution and Biodiversity*, Backhuys  
1313 Publishers.
- 1314 Kravtsova, L. S., L. A. Iziboldina, I. V. Khanaev, and others. 2014. Nearshore benthic blooms of  
1315 filamentous green algae in Lake Baikal. *Journal of Great Lakes Research* **40**: 441–448.  
1316 doi:10.1016/j.jglr.2014.02.019
- 1317 Lapointe, B. E., L. W. Herren, D. D. Debortoli, and M. A. Vogel. 2015. Evidence of sewage-driven  
1318 eutrophication and harmful algal blooms in Florida’s Indian River Lagoon. *Harmful Algae*  
1319 **43**: 82–102. doi:10.1016/j.hal.2015.01.004
- 1320 Lee, S. S., A. M. Paspalof, D. D. Snow, E. K. Richmond, E. J. Rosi-Marshall, and J. J. Kelly. 2016.  
1321 Occurrence and potential biological effects of amphetamine on stream communities.  
1322 *Environmental Science & Technology* **50**: 9727–9735. doi:10.1021/acs.est.6b03717

- 1323 Lin, D., J. Crabtree, I. Dillo, and others. 2020. The TRUST Principles for digital repositories.  
1324 Scientific Data 7: 144. doi:10.1038/s41597-020-0486-7
- 1325 Meyer, M. F., S. G. Labou, A. N. Cramer, M. R. Brousil, and B. T. Luff. 2020. The global lake  
1326 area, climate, and population dataset. Scientific Data 7: 174. doi:10.1038/s41597-020-0517-  
1327 4
- 1328 Meyer, M. F., T. Ozersky, K. H. Woo, and others. 2021. A unified dataset of co-located sewage  
1329 pollution, periphyton, and benthic macroinvertebrate community and food web structure  
1330 from Lake Baikal (Siberia).  
1331 doi:https://doi.org/10.6073/pasta/9554b7f19ddd4a614e854f18be978dca
- 1332 Meyer, M. F., T. Ozersky, K. H. Woo, and others. *Under Review*. Effects of spatially heterogeneous  
1333 lakeside development on nearshore biotic communities in a large, deep, oligotrophic lake  
1334 (Lake Baikal, Siberia).
- 1335 Meyer, M. F., S. M. Powers, and S. E. Hampton. 2019. An evidence synthesis of pharmaceuticals  
1336 and personal care products (PPCPs) in the environment: Imbalances among compounds,  
1337 sewage treatment techniques, and ecosystem types. Environ. Sci. Technol. **53**: 12961–  
1338 12973. doi:10.1021/acs.est.9b02966
- 1339 Meyer, M., T. Ozersky, K. Woo, A. W. E. Galloway, M. R. Brousil, and S. Hampton. 2015. Baikal  
1340 Food Webs. doi:10.17605/OSF.IO/9TA8Z
- 1341 Moore, J. W., D. E. Schindler, M. D. Scheuerell, D. Smith, and J. Frodge. 2003. Lake  
1342 eutrophication at the urban fringe, Seattle region, USA. AMBIO: A Journal of the Human  
1343 Environment **32**: 13–18.

- 1344 Moore, M. V., S. E. Hampton, L. R. Izmet'seva, E. A. Silow, E. V. Peshkova, and B. K. Pavlov.  
1345 2009. Climate change and the world's "Sacred Sea"- Lake Baikal, Siberia. *Bioscience* **59**:  
1346 405–417. doi:10.1525/bio.2009.59.5.8
- 1347 O'Donnell, D. R., P. Wilburn, E. A. Silow, L. Y. Yampolsky, and E. Litchman. 2017. Nitrogen and  
1348 phosphorus colimitation of phytoplankton in Lake Baikal: Insights from a spatial survey and  
1349 nutrient enrichment experiments. *Limnology and Oceanography* **62**: 1383–1392.  
1350 doi:10.1002/lno.10505
- 1351 Pebesma, E. 2018. Simple Features for R: Standardized support for spatial vector data. *The R*  
1352 *Journal* **10**: 439–446. doi:10.32614/RJ-2018-009
- 1353 Powers, S. M., T. W. Bruulsema, T. P. Burt, and others. 2016. Long-term accumulation and  
1354 transport of anthropogenic phosphorus in three river basins. *Nature Geoscience* **9**: 353–356.  
1355 doi:10.1038/ngeo2693
- 1356 R Core Team. 2019. R: A Language and Environment for Statistical Computing.,  
1357 RD:52.24.380-2017. 2018. Nitrate concentration in waters: Photometric methods with Giress  
1358 reagent following stabilization in a cadmium reducer (Массовая концентрация нитратного  
1359 азота в водах: Методика измерений фотометрическим методом с реактивом Грисса  
1360 после восстановления в камиевом редуторе).
- 1361 RD:52.24.383-2018. 2018. Working Document: Concentration of aqueous ammonium: Method for  
1362 measuring with a photometer using indophenol blue (Руководящий Документ: Массовая  
1363 концентрация аммонийного азота в водах: Методика измерений фотометрическим  
1364 методом в виде индофенолового сингео). RD:52.24.383-2018. RD:52.24.383-2018.

- 1365 Richmond, E. K., M. R. Grace, J. J. Kelly, A. J. Reisinger, E. J. Rosi, and D. M. Walters. 2017.  
1366       Pharmaceuticals and personal care products (PPCPs) are ecological disrupting compounds  
1367       (EcoDC). *Elem Sci Anth* **5**: 66. doi:10.1525/elementa.252
- 1368 Richmond, E. K., E. J. Rosi, D. M. Walters, J. Fick, S. K. Hamilton, T. Brodin, A. Sundelin, and M.  
1369       R. Grace. 2018. A diverse suite of pharmaceuticals contaminates stream and riparian food  
1370       webs. *Nature Communications* **9**: 4491. doi:10.1038/s41467-018-06822-w
- 1371 Romera-Castillo, C., M. Pinto, T. M. Langer, X. A. Álvarez-Salgado, and G. J. Herndl. 2018.  
1372       Dissolved organic carbon leaching from plastics stimulates microbial activity in the ocean.  
1373       *Nat Commun* **9**: 1–7. doi:10.1038/s41467-018-03798-5
- 1374 Rosenberger, E. E., S. E. Hampton, S. C. Fradkin, and B. P. Kennedy. 2008. Effects of shoreline  
1375       development on the nearshore environment in large deep oligotrophic lakes. *Freshwater*  
1376       *Biology* **53**: 1673–1691. doi:10.1111/j.1365-2427.2008.01990.x
- 1377 Rosi-Marshall, E. J., D. W. Kincaid, H. A. Bechtold, T. V. Royer, M. Rojas, and J. J. Kelly. 2013.  
1378       Pharmaceuticals suppress algal growth and microbial respiration and alter bacterial  
1379       communities in stream biofilms. *Ecological Applications* **23**: 583–593. doi:10.1890/12-  
1380       0491.1
- 1381 Rosi-Marshall, E. J., and T. V. Royer. 2012. Pharmaceutical compounds and ecosystem function:  
1382       an emerging research challenge for aquatic ecologists. *Ecosystems* **15**: 867–880.  
1383       doi:10.1007/s10021-012-9553-z
- 1384 Sargent, J. R., and S. Falk-Petersen. 1988. The lipid biochemistry of calanoid copepods.  
1385       *Hydrobiologia* **167–168**: 101–114. doi:10.1007/BF00026297

- 1386 Schram, J. B., J. N. Kobelt, M. N. Dethier, and A. W. E. Galloway. 2018. Trophic transfer of  
1387 macroalgal fatty acids in two urchin species: Digestion, egestion, and tissue building. *Front.*  
1388 *Ecol. Evol.* **6**. doi:10.3389/fevo.2018.00083
- 1389 Shaw, L., C. Phung, and M. Grace. 2015. Pharmaceuticals and personal care products alter growth  
1390 and function in lentic biofilms. *Environmental Chemistry* **12**: 301. doi:10.1071/EN14141
- 1391 Slowikowski, K. 2019. ggrepel: Automatically Position Non-Overlapping Text Labels with  
1392 “ggplot2.”
- 1393 Swann, G. E. A., V. N. Panizzo, S. Piccolroaz, and others. 2020. Changing nutrient cycling in Lake  
1394 Baikal, the world’s oldest lake. *PNAS* **117**: 27211–27217. doi:10.1073/pnas.2013181117
- 1395 Taipale, S., U. Strandberg, E. Peltomaa, A. W. E. Galloway, A. Ojala, and M. T. Brett. 2013. Fatty  
1396 acid composition as biomarkers of freshwater microalgae: analysis of 37 strains of  
1397 microalgae in 22 genera and in seven classes. *Aquatic Microbial Ecology* **71**: 165–178.  
1398 doi:10.3354/ame01671
- 1399 Timoshkin, O. A., M. V. Moore, N. N. Kulikova, and others. 2018. Groundwater contamination by  
1400 sewage causes benthic algal outbreaks in the littoral zone of Lake Baikal (East Siberia).  
1401 *Journal of Great Lakes Research*. doi:10.1016/j.jglr.2018.01.008
- 1402 Timoshkin, O. A., D. P. Samsonov, M. Yamamuro, and others. 2016. Rapid ecological change in  
1403 the coastal zone of Lake Baikal (East Siberia): Is the site of the world’s greatest freshwater  
1404 biodiversity in danger? *Journal of Great Lakes Research* **42**: 487–497.  
1405 doi:10.1016/j.jglr.2016.02.011
- 1406 Tong, Y., M. Wang, J. Peñuelas, and others. 2020. Improvement in municipal wastewater treatment  
1407 alters lake nitrogen to phosphorus ratios in populated regions. *Proc Natl Acad Sci USA* **117**:  
1408 11566–11572. doi:10.1073/pnas.1920759117

- 1409 Turetsky, M. R., R. K. Wieder, C. J. Williams, and D. H. Vitt. 2000. Organic matter accumulation,  
1410 peat chemistry, and permafrost melting in peatlands of boreal Alberta. *Écoscience* **7**: 115–  
1411 122. doi:10.1080/11956860.2000.11682608
- 1412 Vendel, A. L., F. Bessa, V. E. N. Alves, A. L. A. Amorim, J. Patrício, and A. R. T. Palma. 2017.  
1413 Widespread microplastic ingestion by fish assemblages in tropical estuaries subjected to  
1414 anthropogenic pressures. *Marine Pollution Bulletin* **117**: 448–455.  
1415 doi:10.1016/j.marpolbul.2017.01.081
- 1416 Volkova, E. A., N. A. Bondarenko, and O. A. Timoshkin. 2018. Morphotaxonomy, distribution and  
1417 abundance of *Spirogyra* (Zygnematophyceae, Charophyta) in Lake Baikal, East Siberia.  
1418 *Phycologia* **57**: 298–308. doi:10.2216/17-69.1
- 1419 Wang, W., and J. Wang. 2018. Investigation of microplastics in aquatic environments: An overview  
1420 of the methods used, from field sampling to laboratory analysis. *TrAC Trends in Analytical*  
1421 *Chemistry* **108**: 195–202. doi:10.1016/j.trac.2018.08.026
- 1422 Welschmeyer, N. A. 1994. Fluorometric analysis of chlorophyll a in the presence of chlorophyll b  
1423 and pheopigments. *Limnol. Oceanogr.* **39**: 1985–1992. doi:10.4319/lo.1994.39.8.1985
- 1424 Wickham, H. 2014. Tidy Data. *Journal of Statistical Software* **59**: 1–23. doi:10.18637/jss.v059.i10
- 1425 Wickham, H., M. Averick, J. Bryan, and others. 2019. Welcome to the tidyverse. *Journal of Open*  
1426 *Source Software* **4**: 1686. doi:10.21105/joss.01686
- 1427 Wilke, C. O. 2019. cowplot: Streamlined Plot Theme and Plot Annotations for “ggplot2.”
- 1428 Wilkinson, M. D., M. Dumontier, Ij. J. Aalbersberg, and others. 2016. The FAIR Guiding  
1429 Principles for scientific data management and stewardship. *Sci Data* **3**.  
1430 doi:10.1038/sdata.2016.18

1431     Yang, Y., W. Song, H. Lin, W. Wang, L. Du, and W. Xing. 2018. Antibiotics and antibiotic  
1432             resistance genes in global lakes: A review and meta-analysis. *Environment International*  
1433             **116**: 60–73. doi:10.1016/j.envint.2018.04.011

1434     Yoshida, T., T. Sekino, M. Genkai-Kato, and others. 2003. Seasonal dynamics of primary  
1435             production in the pelagic zone of southern Lake Baikal. *Limnology* **4**: 53–62.  
1436             doi:10.1007/s10201-002-0089-3

1437  
1438  
1439

**Acknowledgements**

We would like to thank the faculty, students, staff, and mariners of the Irkutsk State University's Biological Research Institute Biostation for their expert field, taxonomic, and laboratory support; Marianne Moore and Bart De Stasio for helpful advice; the researchers and students of the Siberian Branch of the Russian Academy of Sciences Limnological Institute for expert taxonomic and logistical assistance; Oleg A. Timoshkin, Tatiana Ya. Sitnikova, Irina V. Mekhanikova, Nina A. Bondorenko, Ekaterina Volkova, and Vadim V. Takhteev for offering insights and taxonomic training throughout the development of this project. We would also like to thank Dag O. Hessen and an anonymous reviewer for helping us improve the clarity of our data article as well as the reproducibility and transparency of our data products. Funding was provided by the National Science Foundation (NSF-DEB-1136637) to S.E.H., a Fulbright Fellowship to M.F.M., a NSF Graduate Research Fellowship to M.F.M. (NSF-DGE-1347973), and Russian Ministry of Science and Education (N FZZE-2020-0026; N FZZE-2020-0023). This work serves as one chapter of M.F.M.'s doctoral dissertation in Environmental and Natural Resource Sciences at Washington State University.



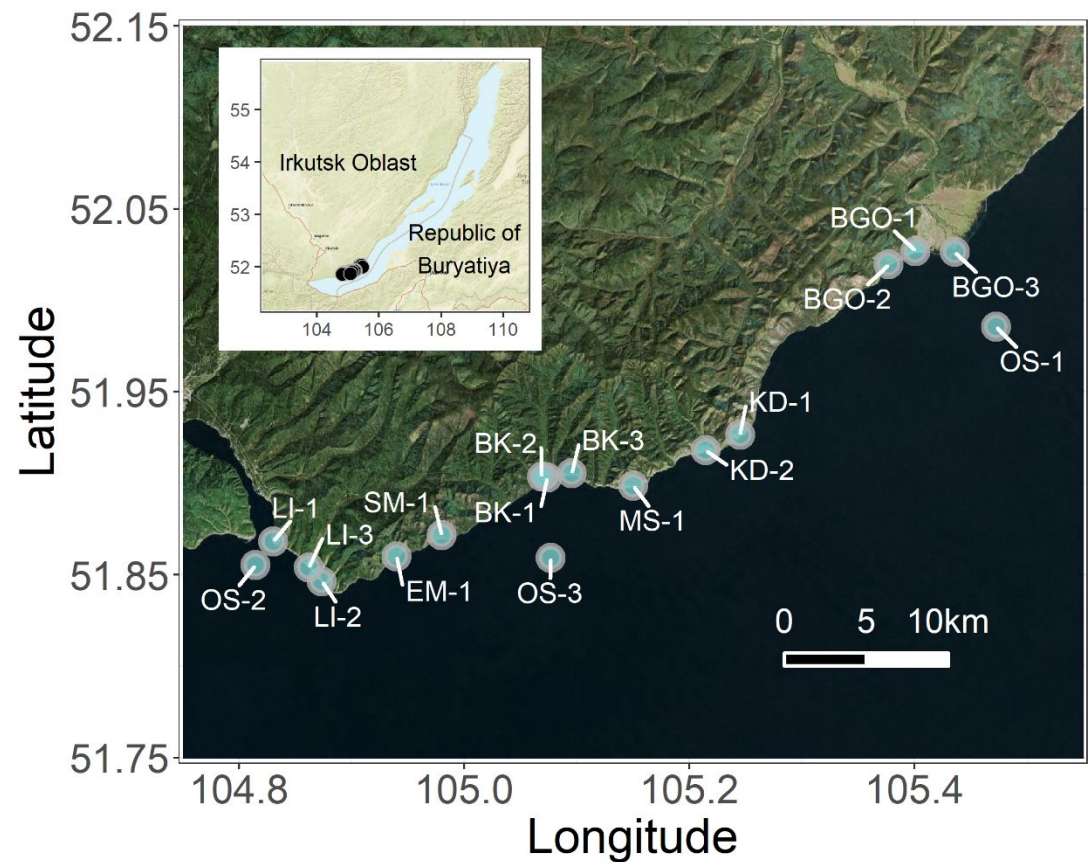


Figure 1: Map of all sampling locations with sites labeled with unique alphanumeric code. The entire transect included three developed sites (i.e., Listvyanka (LI), Bolshie Koty (BK), Bolshoe Goloustnoe (BGO)). Three offshore sites (OS) were also sampled to compare pelagic sewage signals to those in the littoral. Sites without adjacent lakeside development included Emelyanikha Bay (EM), Maloe Kadilnoe (KD), Mys Soboliny (MS), Sredny Mys (SM). Littoral sampling locations were all 8.90-20.75 m from shore and at a depth approximately of 0.75 m, whereas pelagic sites were approximately 2-5 km from shore and ranged in depth from 900 to 1300 m. This map was created using the R statistical environment (R Core Team 2019) and the tidyverse (Wickham et al. 2019), OpenStreetMap (Fellows and Stotz 2019), ggpubr (Kassambara 2019), cowplot (Wilke 2019), ggson (Baquero 2019), and ggrepel (Slowikowski 2019) packages. This map was produced using data from © OpenStreetMap contributors (<https://www.openstreetmap.org/copyright>), which is licensed under the Open Data Commons Open Database License (ODbL) by the

OpenStreetMap Foundation (OSMF). Base map and data from OpenStreetMap and OSMF were created using the © ESRI (inset map) and © 2021 Microsoft Corporation Earthstar Geographics SIO “bing” (zoomed-in map) tiles.

Site	Latitude	Longitude	Depth (m)	Distance to shore (m)
BK-1	51.90316	105.074	0.7	10
BK-2	51.90365	105.069	0.9	17.5
BK-3	51.90536	105.0957	0.8	10
BGO-1	52.02693	105.401	0.9	18
BGO-2	52.0197	105.3771	1.1	14
BGO-3	52.02649	105.4358	0.7	21
OS-1	51.98559	105.4724	900	NA
KD-1	51.92646	105.245	0.8	20.75
KD-2	51.91807	105.2146	0.9	14.5
MS-1	51.89863	105.1502	0.6	10.5
SM-1	51.87152	104.9801	0.9	11.5
LI-1	51.86825	104.8304	0.6	8.9
LI-2	51.84626	104.8736	0.8	9.4
LI-3	51.85407	104.8622	0.7	9.25
EM-1	51.86005	104.94	0.7	15.5
OS-2	51.8553	104.8148	1300	NA
OS-3	51.85911	105.0769	1400	5000

Table 1: Locational information for each of the 17 sampling stations. “OS” refers to pelagic locations (i.e., “Offshore”), whereas other site abbreviations refer to littoral sampling locations.

Table 2: Summary table of algal and macroinvertebrate data within the dataset. Although fatty acids contain data on *Hyalella* spp., these specimens were likely misidentified in the field before processing. For consistency and detailing the breadth of fatty acid profiles among Baikal's littoral amphipods, we have included them in the dataset, but caution should be taken when considering these fatty acids explicitly as those representative of *Hyalella* spp.

Variable	Course Taxonomic Grouping	Finest Taxonomic Group in Dataset
Abundance Estimates	Amphipoda	<i>Brandtia latissima</i> subsp. (Dorogostaiskii 1930; Dybowsky 1874) <i>Brandtia parasitica parasitica</i> (Dybowsky 1874) <i>Cryptoropus inflatus</i> (Dybowsky 1874) <i>Cryptoropus pachytus</i> (Dybowsky 1874) <i>Cryptoropus rugosus</i> (Dybowsky 1874) <i>Eulimnogammarus capreolus</i> (Dybowsky 1874) <i>Eulimnogammarus cruentus</i> (Dorogostaiskii 1930) <i>Eulimnogammarus cyaneus</i> (Dybowsky 1874) <i>Eulimnogammarus grandimanus</i> (Bazikalova 1945) <i>Eulimnogammarus maacki</i> (Gerstfeldt 1858) <i>Eulimnogammarus marituji</i> (Bazikalova 1945) <i>Eulimnogammarus verucossus</i> (Gerstfeldt 1858) <i>Eulimnogammarus viridis viridis</i> (Dybowsky 1874) <i>Eulimnogammarus vittatus</i> (Dybowsky 1874) <i>Pallasea brandtia brandita</i> (Dybowsky 1874) <i>Pallasea brandtii tenera</i> (Sovinskii 1930) <i>Pallasea cancelloides</i> (Gerstfeldt 1858) <i>Pallasea cancellus</i> (Pallas 1776) <i>Pallasea viridis</i> (Garjajev 1901) <i>Poekilogammarus crassimus</i> (Sovinskii 1915) <i>Poekilogammarus ehippiatus</i> (Dybowsky 1874) <i>Poekilogammarus megonychus perpolitus</i> (Takhteev 2002) <i>Poekilogammarus pictus</i> (Dybowsky 1874)
	Molluska	Acroloxidae Baicaliidae Benedictidae Maackia Planorbidae Valvatidae
	Other Macroinvertebrates	Asellidae

		Caddisflies Hirudinea Planaria
	Benthic Algae	Diatom <i>Ulothrix</i> spp. <i>Spirogyra</i> spp. Tetrasporales
Stable Isotopes	Amphipoda	<i>Eulimnogammarus cyaneus</i> (Dybowsky 1874) <i>Eulimnogammarus verucossus</i> (Gerstfeldt 1858) <i>Eulimnogammarus vittatus</i> (Dybowsky 1874) <i>Pallasea cancellus</i> (Pallas 1776)
	Benthic Algae	Periphyton
Fatty Acids	Amphipoda	<i>Eulimnogammarus cyaneus</i> (Dybowsky 1874) <i>Eulimnogammarus verucossus</i> (Gerstfeldt 1858) <i>Eulimnogammarus vittatus</i> (Dybowsky 1874) <i>Hyaella</i> spp. <i>Pallasea cancellus</i> (Pallas 1776)
	Molluska	Processed in composite and not identified to family.
	Benthic Algae	Periphyton <i>Draparnaldia</i> spp.

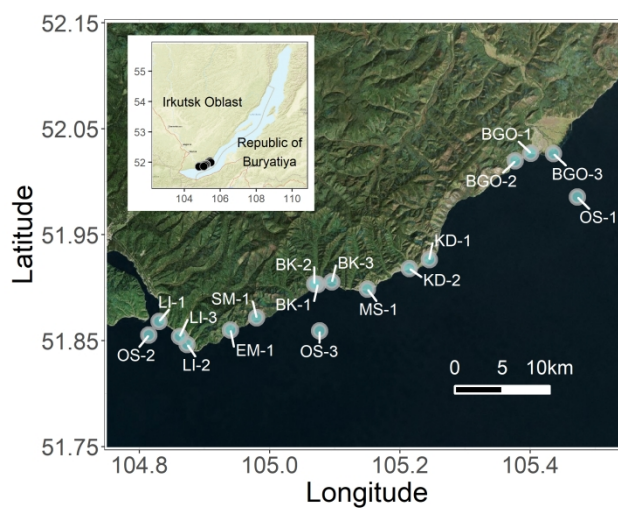


Figure 1: Map of all sampling locations with sites labeled with unique alphanumeric code. The entire transect included three developed sites (i.e., Listvyanka (LI), Bolshie Koty (BK), Bolshoe Goloustnoe (BGO)). Three offshore sites (OS) were also sampled to compare pelagic sewage signals to those in the littoral. Sites without adjacent lakeside development included Emelyanikha Bay (EM), Maloe Kadilnoe (KD), Mys Soboliny (MS), Sredny Mys (SM). Littoral sampling locations were all 8.90-20.75 m from shore and at a depth approximately of 0.75 m, whereas pelagic sites were approximately 2-5 km from shore and ranged in depth from 900 to 1300 m. This map was created using the R statistical environment (R Core Team 2019) and the tidyverse (Wickham et al. 2019), OpenStreetMap (Fellows and Stotz 2019), ggpubr (Kassambara 2019), cowplot (Wilke 2019), ggsm (Baquero 2019), and ggrepel (Slowikowski 2019) packages. This map was produced using data from © OpenStreetMap contributors (<https://www.openstreetmap.org/copyright>), which is licensed under the Open Data Commons Open Database License (ODbL) by the OpenStreetMap Foundation (OSMF). Base map and data from OpenStreetMap and OSMF were created using the © ESRI (inset map) and © 2021 Microsoft Corporation Earthstar Geographics SIO "bing" (zoomed-in map) tiles.

774x387mm (118 x 118 DPI)

Site	Latitude	Longitude	Depth (m)	Distance to shore (m)
BK-1	51.90316	105.074	0.7	10
BK-2	51.90365	105.069	0.9	17.5
BK-3	51.90536	105.0957	0.8	10
BGO-1	52.02693	105.401	0.9	18
BGO-2	52.0197	105.3771	1.1	14
BGO-3	52.02649	105.4358	0.7	21
OS-1	51.98559	105.4724	900	NA
KD-1	51.92646	105.245	0.8	20.75
KD-2	51.91807	105.2146	0.9	14.5
MS-1	51.89863	105.1502	0.6	10.5
SM-1	51.87152	104.9801	0.9	11.5
LI-1	51.86825	104.8304	0.6	8.9
LI-2	51.84626	104.8736	0.8	9.4
LI-3	51.85407	104.8622	0.7	9.25
EM-1	51.86005	104.94	0.7	15.5
OS-2	51.8553	104.8148	1300	NA
OS-3	51.85911	105.0769	1400	5000

Table 1: Locational information for each of the 17 sampling stations. “OS” refers to pelagic locations (i.e., “Offshore”), whereas other site abbreviations refer to littoral sampling locations.

Table 2: Summary table of algal and macroinvertebrate data within the dataset. Although fatty acids contain data on *Hyaella* spp., these specimens were likely misidentified in the field before processing. For consistency and detailing the breadth of fatty acid profiles among Baikal's littoral amphipods, we have included them in the dataset, but caution should be taken when considering these fatty acids explicitly as those representative of *Hyaella* spp.

Variable	Course Taxonomic Grouping	Finest Taxonomic Group in Dataset
Abundance Estimates	Amphipoda	<i>Brandtia latissima</i> subspp. (Dorogostaiskii 1930; Dybowsky 1874) <i>Brandtia parasitica parasitica</i> (Dybowsky 1874) <i>Cryptoropus inflatus</i> (Dybowsky 1874) <i>Cryptoropus pachytus</i> (Dybowsky 1874) <i>Cryptoropus rugosus</i> (Dybowsky 1874) <i>Eulimnogammarus capreolus</i> (Dybowsky 1874) <i>Eulimnogammarus cruentus</i> (Dorogostaiskii 1930) <i>Eulimnogammarus cyaneus</i> (Dybowsky 1874) <i>Eulimnogammarus grandimanus</i> (Bazikalova 1945) <i>Eulimnogammarus maacki</i> (Gerstfeldt 1858) <i>Eulimnogammarus marituji</i> (Bazikalova 1945) <i>Eulimnogammarus verucossus</i> (Gerstfeldt 1858) <i>Eulimnogammarus viridis viridis</i> (Dybowsky 1874) <i>Eulimnogammarus vittatus</i> (Dybowsky 1874) <i>Pallasea brandtia brandita</i> (Dybowsky 1874) <i>Pallasea brandtii tenera</i> (Sovinskii 1930) <i>Pallasea cancelloides</i> (Gerstfeldt 1858) <i>Pallasea cancellus</i> (Pallas 1776) <i>Pallasea viridis</i> (Garjajev 1901)



		<i>Poekilogammarus crassimus</i> (Sovinskii 1915) <i>Poekilogammarus ehippiatus</i> (Dybowsky 1874) <i>Poekilogammarus megonychus perpolitus</i> (Takhteev 2002) <i>Poekilogammarus pictus</i> (Dybowsky 1874)
	Molluska	Acroloxidae Baicaliidae Benedictidae Maackia Planorbidae Valvatidae
	Other Macroinvertebrates	Asellidae Caddisflies Hirudinea Planaria
	Benthic Algae	Diatom <i>Ulothrix</i> spp. <i>Spirogyra</i> spp. Tetrasporales
Stable Isotopes	Amphipoda	<i>Eulimnogammarus cyaneus</i> (Dybowsky 1874) <i>Eulimnogammarus verucossus</i> (Gerstfeldt 1858) <i>Eulimnogammarus vittatus</i> (Dybowsky 1874) <i>Pallasea cancellus</i> (Pallas 1776)
	Benthic Algae	Periphyton
Fatty Acids	Amphipoda	<i>Eulimnogammarus cyaneus</i> (Dybowsky 1874)

		<i>Eulimnogammarus verucossus</i> (Gerstfeldt 1858) <i>Eulimnogammarus vittatus</i> (Dybowsky 1874) <i>Hyaella</i> spp. <i>Pallasea cancellus</i> (Pallas 1776)
	Molluska	Processed in composite and not identified to family.
	Benthic Algae	Periphyton <i>Draparnaldia</i> spp.